On the Secondary Source Type Mismatch in Wave Field Synthesis Employing Circular Distributions of Loudspeakers

Jens Ahrens and Sascha Spors

Deutsche Telekom Laboratories, Technische Universität Berlin, Ernst-Reuter-Platz 7, 10587 Berlin, Germany

Correspondence should be addressed to Jens Ahrens (`jens.ahrens@telekom.de`)

ABSTRACT

The theory of wave field synthesis has been formulated for linear and planar arrays of loudspeakers but has been found to be also applicable with arbitrary convex loudspeaker contours with acceptable error. The main source of error results from the fact that the required properties of the employed loudspeakers are dictated by the Neumann Green's function of the array geometry under consideration. For non-linear and non-planar arrays a systematic error arises which is a result of the mismatch between the spatio-temporal transfer function of the loudspeakers and the Neumann Green's function of the loudspeaker contour under consideration. We investigate this secondary source type mismatch for the case of circular distributions of loudspeakers.

1. INTRODUCTION

Wave field synthesis (WFS) is an approach to the physical reproduction of sound fields over an extended receiver area by means of arrays of secondary sources, i.e. loudspeakers. The underlying theory was initially derived from the Rayleigh integrals which require the employed secondary source distributions to be linear in the two-dimensional case or to be planar in the three-dimensional case, e.g. [1]. A reformulation of the theory based on the Kirchhoff-Helmholtz integral revealed that also curved distributions can be employed [2, 3]. The initial Kirchhoff-Helmholtz formulation requires that the listening area is enclosed by a layer of monopole secondary sources and by a layer of dipole secondary sources. The former can be approximated by loudspeakers with closed cabinets. The latter are hardly realizable by commonly available loudspeakers.

It was shown that the dipole layer can be waived

when the sound field outside the secondary source distribution is not required to be zero as it is the case in the initial Kirchhoff-Helmholtz formulation. As a consequence, the secondary source contour has to be convex. The convexity is necessary in order to avoid that sound emitted from a particular secondary source can re-enter the receiver area. In this dipoleless formulation, the employed secondary sources are required to exhibit a spatio-temporal transfer function which is equal to the Neumann Green's function of the geometry under consideration.

Omnidirectional secondary sources can be used to imitate such a Neumann Green's function in the case of linear/planar arrays by doubling the amplitude of the driving signal. For curved distributions the employed secondary sources have to exhibit a complex spatio-temporal transfer function which depends on the individual geometry of the secondary source distribution under consideration in order to fulfil the theoretical requirements. Loudspeakers which exhibit such properties are commonly not available. Therefore, loudspeakers are used whose spatio-temporal transfer function is modeled to be omnidirectional. This fact introduces a systematic theoretic error for non-planar/non-linear distributions. We term this error being a consequence of the *secondary source type mismatch*.

An additional error is introduced in practical implementations of wave field synthesis due to the fact that typically loudspeakers which are omnidirectional in three dimensions are employed for two-dimensional reproduction. We term this error being a consequence of the *dimensionality mismatch* of the secondary sources.

Such a situation is referred to as 2.5-dimensional reproduction. In order to investigate the secondary source type mismatch independently from the 2.5D errors, we assume a two-dimensional scenario in which the employed secondary sources are omnidirectional in a two-dimensional sense. Despite the above described drawbacks, WFS is a very popular technique due to the fact that the loudspeaker driving functions for simple wave fields like plane and spherical waves can be very efficiently implemented. This circumstance makes realtime implementation straightforward.

Practical implementations of wave field synthesis typically employ piecewise linear or circular distri-

butions of secondary sources. In either case, previous investigations of the secondary source type mismatch are restricted to numerical simulations and informal listening. In this contribution, we concentrate on the case of circular distributions of omnidirectional secondary sources.

The analysis is based on a comparison of the properties of WFS and the theoretically correct solution. The theoretically correct solution for the secondary source driving signals has recently been derived by several authors in the context of higher order Ambisonics, e.g. [4, 5, 6, 7].

2. NOMENCLATURE

For convenience, we restrict our considerations to two spatial dimensions. This means in this context that a sound field under consideration is independent from one of the spatial coordinates, i.e. $P(x, y, z, \omega) = P(x, y, \omega)$. Refer to Sec. 3 for an outline of the consequences of this assumption.

The two-dimensional position vector in Cartesian coordinates is given as $\mathbf{x} = [x \ y]^T$. The Cartesian coordinates are linked to the polar coordinates via $x = r \cos \alpha$ and $y = r \sin \alpha$. Refer to the coordinate system depicted in Fig. 1.

The acoustic wavenumber is denoted by k. It is related to the temporal frequency by $k^2 = \left(\frac{\omega}{c}\right)^2$ with ω being the radial frequency and c the speed of sound. Outgoing monochromatic cylindrical waves are denoted by $H_0^{(2)}(\frac{\omega}{c}r)$. The imaginary unit is denoted by j $(j = \sqrt{-1})$.
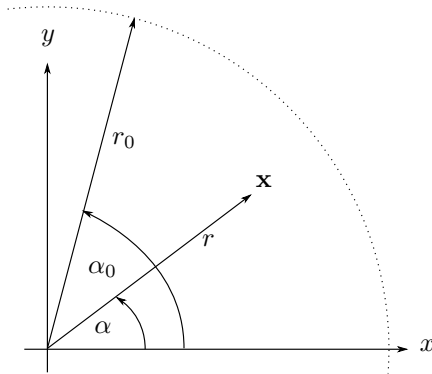
A propagating two-dimensional sound field $P(\mathbf{x}, \omega)$ can be by described by its circular harmonics expansion as [8]

$$P(\mathbf{x}, \omega) = \sum_{\nu=-\infty}^{\infty} \underbrace{\breve{P}_\nu(\omega) J_\nu \left(\frac{\omega}{c} r\right)}_{= \mathring{P}_\nu(r, \omega)} e^{j\nu\alpha} , \qquad (1)$$

whereby $J_\nu(\cdot)$ denotes the ν-th order Bessel function.

The Fourier series expansion coefficients $\mathring{P}_\nu(r, \omega)$ of $P(\mathbf{x}, \omega)$ can be obtained via [8]

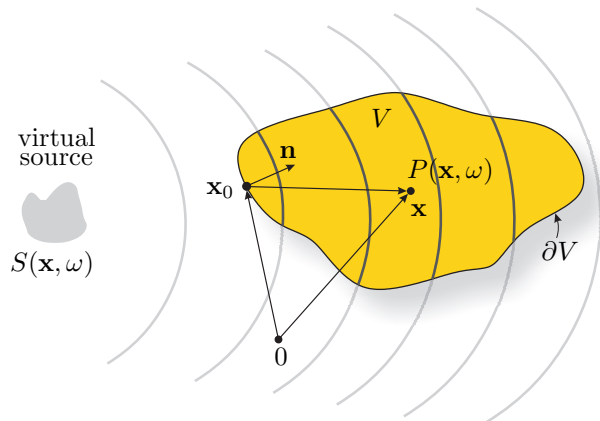$$\mathring{P}_\nu(r, \omega) = \frac{1}{2\pi} \int_0^{2\pi} P(\mathbf{x}, \omega) e^{-j\nu\alpha} \, d\alpha . \qquad (2)$$

Fig. 1: The coordinate system used in this paper. The dashed line indicates the secondary source distribution.

Fig. 2: Illustration of the geometry used for the Kirchhoff-Helmholtz integral (3).

3. THEORY

We briefly revisit the theory of sound field reproduction relevant to the presented investigations in this section. Refer to [3, 6, 9] for an extensive treatment. The sample scenario under consideration in this paper is a virtual plane wave reproduced by a circular distribution of secondary line sources (i.e. purely 2D reproduction). The choice of a plane wave is justified since arbitrary propagating wave fields can be described by an appropriate superposition of plane waves [8].

The secondary line sources are positioned perpendicular to the target plane (the receiver plane). Our approach is therefore not directly implementable since loudspeakers exhibiting the properties of line sources are commonly not available. Real-world implementations usually employ loudspeakers with closed cabinets as secondary sources. The properties of these loudspeakers are more accurately modeled by point sources.

The main motivation to focus on two dimensions is to keep the mathematical formulation simple in order to illustrate the fundamental properties. The extension both to three-dimensional reproduction (i.e. spherical arrays of secondary point sources) and to two-dimensional reproduction employing circular arrangements of secondary point sources (*2.5-dimensional reproduction*) is straightforward and a general treatment thereof can be found e.g. in [3, 6].

3.1. The Kirchhoff-Helmholtz Integral

A loudspeaker system surrounding the listener can be regarded as an inhomogeneous boundary condition. The solution of the homogeneous wave equation for a bounded region V with respect to inhomogeneous boundary conditions is given by the Kirchhoff-Helmholtz integral [8]

$$P(\mathbf{x}, \omega) = -\oint_{\partial V} \left(G(\mathbf{x}|\mathbf{x}_0, \omega) \frac{\partial}{\partial \mathbf{n}} P(\mathbf{x}, \omega)\Big|_{\mathbf{x}=\mathbf{x}_0} - P(\mathbf{x}_0, \omega) \frac{\partial}{\partial \mathbf{n}} G(\mathbf{x}|\mathbf{x}_0, \omega) \right) dS_0 ; \quad (3)$$

where $P(\mathbf{x}, \omega)$ denotes the pressure field inside a bounded region V enclosed by the boundary ∂V ($\mathbf{x} \in V$), $G(\mathbf{x}|\mathbf{x}_0, \omega)$ a suitably chosen Green's function, $P(\mathbf{x}_0, \omega)$ the acoustic pressure at the boundary ∂V ($\mathbf{x}_0 \in \partial V$) and $\mathbf{n}$ the inward pointing normal vector of ∂V. The abbreviation $\frac{\partial}{\partial \mathbf{n}}$ denotes the directional gradient in direction of the normal vector $\mathbf{n}$. The wave field $P(\mathbf{x}, \omega)$ outside of V is zero and V is assumed to be source-free. Figure 2 illustrates the geometry.

For sound reproduction typically free-field propagation within V is assumed. This implies that V is free of any objects and that the boundary ∂V does not restrict propagation. The Green's function is then given as the free-field solution of the wave equation and is referred to as *free-field Green's function* $G_0(\mathbf{x}|\mathbf{x}_0, \omega)$. The free-field Green's function can be interpreted as the spatio-temporal transfer func-

tion of a monopole placed at the point $\mathbf{x}_0$ and its directional gradient as the spatio-temporal transfer function of a dipole at the point $\mathbf{x}_0$, whose main axis points towards $\mathbf{n}$.

Equation (3) states that if the Green's function is realized by a continuous distribution of appropriately driven monopole and dipole sources which are placed on the boundary ∂V, the wave field within V is fully determined by these sources. This principle can be used for sound reproduction as will be illustrated in the following. In this context the monopole and dipole sources on the boundary are referred to as (monopole/dipole) *secondary sources.*

The Kirchhoff-Helmholtz integral implies that accurate sound field reproduction can be realized if a distribution of secondary monopole and dipole sources on the boundary ∂V of the listening area V is driven by the directional gradient and the pressure of the wave field of the virtual source $S(\mathbf{x}, \omega)$, respectively. It is desirable for a practical implementation to discard one of the two types of secondary sources. Monopole sources can be realized reasonably well by loudspeakers with closed cabinets and it is therefore desirable to discard the secondary dipole sources.

3.2. Neumann Green's Function

The second term in the Kirchhoff-Helmholtz integral (3), representing the dipole secondary sources, can be eliminated by changing the Green's function used in the Kirchhoff-Helmholtz integral [8]. Depending on the situation, this may also imply that other sources than monopoles have to be used as secondary sources.

The basic concept is to use a Neumann Green's function in order to eliminate the dipole secondary sources. A Neumann Green's function has to obey the following condition

$$\frac{\partial}{\partial \mathbf{n}} G_{\mathrm{N}}(\mathbf{x}|\mathbf{x}_0, \omega)\Big|_{\mathbf{x}_0 \in \partial V} = 0 \ . \qquad (4)$$

Introducing the definition of the Neumann Green's function (4) into the Kirchhoff-Helmholtz integral (3) yields the reproduced wave field as

$$P(\mathbf{x}, \omega) = -\oint_{\partial V} \frac{\partial}{\partial \mathbf{n}} S(\mathbf{x}, \omega)\Big|_{\mathbf{x} = \mathbf{x}_0} G_{\mathrm{N}}(\mathbf{x}|\mathbf{x}_0, \omega) \ dS_0 \ .$$
$$(5)$$

The explicit form of the Neumann Green's function depends on the geometry of the boundary ∂V. A

closed form solution can only be found for rather simple geometries like spheres and planar boundaries [10]. The boundary ∂V is implicitly modeled as an acoustically rigid surface for the secondary sources. This is a consequence of the condition given by (4).

Equation (5) states, that if the Neumann Green's function can be realized by a physically existing secondary source, i.e. if a loudspeakers whose spatio-temporal transfer function equals the Neumann Green's function $G_{\mathrm{N}}(\cdot)$ for the given geometry, then the driving signal is simply given by the directional gradient of the virtual source. Depending on the explicit form of the Neumann Green's function such secondary sources may be impossible to realize in practice.

3.3. Wave Field Synthesis

For a planar/linear boundary ∂V, a suitable Neumann Green's function can be derived by adding an image source with respect to the boundary ∂V to the free-field Green's function [8]. This solution fulfils the condition (4) due to the specialized geometry. In this case the Neumann Green's function is given as

$$G_{\mathrm{N}}(\mathbf{x}|\mathbf{x}_0, \omega)\Big|_{\mathbf{x}_0 \in \partial V} = 2 \ G_0(\mathbf{x}|\mathbf{x}_0, \omega) \ , \qquad (6)$$

whereby (6) only holds inside the target half-space. Hence, for the linear/planar case $G_{\mathrm{N}}(\mathbf{x}|\mathbf{x}_0, \omega)$ is equal to a monopole source with double strength. Introducing $G_{\mathrm{N}}(\mathbf{x}|\mathbf{x}_0, \omega)$ into the Kirchhoff-Helmholtz integral derives the first Rayleigh integral, which is the basis for the traditional derivation of WFS [11]. However, this theoretical basis holds only for linear/planar secondary source distributions. In WFS, it is assumed that (6) holds also approximately for other geometries [2].

The application of the Neumann Green's function for linear/planar boundaries (6) in order to eliminate the secondary dipole sources for arbitrary secondary source contours ∂V has two consequences:

1. the wave field outside of V will not be zero, and

2. the reproduced wave field will not match the virtual source field exactly within V.

The first consequence implies that the boundary ∂V has to be convex, so that no contributions from the wave field outside of the listening area V propagate

back into the listening area. The second is a consequence of approximating the Neumann Green's function for non-linear/non-planar geometries using (6). Using this Neumann Green's function for curved secondary source contours leads to artifacts in the reproduced wave field.

As a consequence of modeling the boundary as acoustically rigid (refer to Sec. 3.2), an artificial reflection on the boundary is produced. This artificial reflection is also termed *secondary diffraction* in the context of scattering problems [12].

One possibility to reduce the energy of the secondary diffraction is to mute those secondary sources whose normal vector $\mathbf{n}$ does not coincide with the local propagation direction of the virtual wave field.

Following this concept, the sound field reproduced by a continuous circular distribution of secondary monopole line sources and with radius r_0 reads

$$P_{\mathrm{WFS}}(\mathbf{x}, \omega) =$$
$$\int_0^{2\pi} D_{\mathrm{WFS}}(\alpha_0, \omega)\, G_0(\alpha - \alpha_0, r, r_0, \omega)\, r_0\, d\alpha_0 \; ; \quad (7)$$

with

$$D_{\mathrm{WFS}}(\mathbf{x}_0, \omega) = -2a(\mathbf{x}_0)\frac{\partial}{\partial \mathbf{n}} S(\mathbf{x}, \omega)\Big|_{\mathbf{x}=\mathbf{x}_0} . \quad (8)$$

$a(\mathbf{x}_0)$ denotes a suitably chosen window function. This function takes care that only those secondary sources are active where the local propagation direction of the virtual source's sound field at the position $\mathbf{x}_0$ has a positive component in direction of the normal vector $\mathbf{n}$ of the secondary source. It was proposed in [13] to formulate this condition analytically on basis of the acoustic intensity vector.

For an arbitrarily shaped boundary ∂V, the reproduced wave field will not exactly match the virtual source field $S(\mathbf{x}, \omega)$ within V. The analysis of the error introduced due to the application of a Neumann Green's function for a linear/planar boundary on circular/cylindrical boundaries in combination with the necessary window function $a(\mathbf{x}_0)$ is the subject of this paper. For convenience, we investigate the above described error for the reproduction of a virtual plane wave. Conclusions for complex sound fields can be drawn from plane waves since arbitrary sound fields can be described by an appropriate superposition of plane waves [8].

For the considered scenario of a virtual plane wave reproduced by a continuous distribution of secondary monopole line sources, the driving function $D_{\mathrm{WFS}}(\alpha, \omega)$ is explicitly given by

$$D_{\mathrm{WFS}}(\alpha, \omega) = -2a(\alpha)jk_{\mathrm{pw}}\cos(\theta_{\mathrm{pw}} - \alpha)\times$$
$$\times\, e^{-jk_{\mathrm{pw}}r_0\cos(\theta_{\mathrm{pw}} - \alpha)} , \quad (9)$$

whereby $a(\alpha)$ is given by

$$a(\alpha) = H\left(\theta_{\mathrm{pw}} + \frac{\pi}{2}\right) - H\left(\theta_{\mathrm{pw}} + \frac{3\pi}{2}\right) , \quad (10)$$

with $H(\cdot)$ denoting the Heaviside step function [14].

3.4. Interpretation of WFS in terms of equivalent scattering problem

As pointed out in [15], it can be helpful to approach WFS by considering the equivalent problem of scattering of sound waves at a sound-soft object whose geometry is equal to that of the secondary source distribution. Sound-soft objects exhibit ideal pressure release boundaries. This condition is referred to as *homogeneous Dirichlet boundary condition*.

When the wavelength $\lambda = {}^{2\pi}/k$ of the wave field under consideration is much smaller than the dimensions of the scattering object the so-called *Kirchhoff* or *physical optics approximation* [12] can be applied. The surface of the scattering object is divided into a region which is *illuminated* by the incident wave, and a *shadowed* area. The problem under consideration is then reduced to far-field scattering off the illuminated region whereby the surface of the scattering object is assumed to be locally plane.

It can be shown that the region covered by the window function $a(\mathbf{x}_0)$ applied in WFS, as derived in [13] on the basis of the sound intensity vector, does indeed correspond to the illuminated region in the equivalent scattering problem. Additionally, by applying (6) it also assumed in WFS that the secondary source distribution is locally plane.

We can therefore conclude that WFS employing non-linear/non-planar secondary source distributions constitutes a physical optics approximation of sound field reproduction.

In order to validate the concept of WFS we have to investigate whether the requirements for application of the physical optics approximation are met.

As stated above, the wavelength λ has to be much smaller than the dimensions of the secondary source distribution under consideration.

In the analysis in Sec. 4, we primarily consider a secondary source distribution of radius $r_0 = 1.5$ m. This radius corresponds to the wavelength of around 230 Hz. That means that for frequencies much larger than 230 Hz, the physical optics approximation is justified and it is expected that the error is negligible.

However, in sound field reproduction applications, signals with a frequency of around 230 Hz and lower do indeed frequently occur. In this case we have to expect considerable artifacts.

3.5. Exact solution

In order to assess the accuracy of WFS we have to know the exact solution to the problem under consideration. This exact solution was achieved in the context of higher order Ambisonics. The latter approach can be shown to be also a monopole-only formulation of the Kirchhoff-Helmholtz integral [9]. Although a number of variants of Ambisonics exists (refer to Sec. 1), we choose the approach presented by the authors in [6] for convenience. Refer to [9] for a more extensive outline of the physical basis and of alternative formulations.

The physical fundament of the revisited approach is the concept of *single-layer potentials* [12], and it can be seen as an analytical formulation of what is known as higher order Ambisonics (see e.g. [16]). Source-free solutions to the Helmholtz equation can be represented by a single-layer potential which encloses the receiver area [8].

In WFS, the driving function for a given secondary source is calculated via the directional gradient of the virtual sound field (refer to (8)). In the Ambisonics context, (7) which constitutes an integral equation of first kind, is explicitly solved for the driving function.

Recall (7) which is given by

$$P(\mathbf{x},\omega) = \int_0^{2\pi} D_{\mathrm{exact}}(\alpha_0,\omega)\, G(\alpha-\alpha_0,r,r_0,\omega)\, r_0\, d\alpha_0 .$$

$$(11)$$

Again, $P(\mathbf{x},\omega)$ denotes the reproduced sound field, $D_{\mathrm{exact}}(\alpha_0,\omega)$ the driving function for the secondary source situated at $\mathbf{x}_0$, and $G(\alpha-\alpha_0,r,r_0,\omega)$ its two-

dimensional spatio-temporal transfer function. In the classical single-layer formulation, $D(\alpha_0,\omega)$ is referred to as density of the potential.

A fundamental property of (11) is its inherent
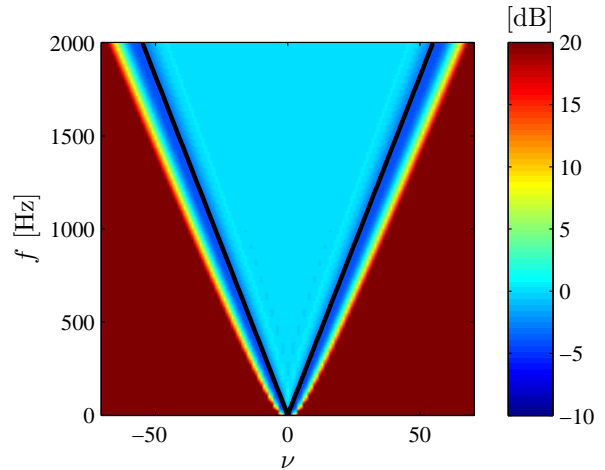
Fig. 4: $20 \cdot \log_{10} |\mathring{P}_{\nu,\mathrm{WFS}}(\omega)/\mathring{P}_{\nu,\mathrm{exact}}(\omega)|$. $r_0 = 1.5$ m. The values are clipped as indicated by the colorbars.

non-uniqueness and ill-posedness [17]. I.e. in certain situations, the solution is undefined and so-called *critical* or *forbidden frequencies* arise. The forbidden frequencies are discrete and represent the resonances of the cavity under consideration. However, there are indications that the forbidden frequencies are only of minor relevance when practical implementations are considered [8].

Equation (11) constitutes a circular convolution and therefore the convolution theorem

$$\mathring{P}_\nu(r,\omega) = 2\pi r_0\, \mathring{D}_\nu(\omega)\, \mathring{G}_\nu(r,\omega) \qquad (12)$$

applies [18]. $\mathring{P}_\nu(r,\omega)$, $\mathring{D}_\nu(\omega)$, and $\mathring{G}_\nu(r,\omega)$ denote the Fourier series expansion coefficients of $P(\mathbf{x},\omega)$, $D(\alpha,\omega)$, and $G\left(\mathbf{x} - [r_0\ 0]^T\right)$[1].

---

[1]Note that the coefficients $\mathring{G}_\nu(r,\omega)$ as used throughout this paper assume that the secondary source is situated at the position $(r = r_0, \alpha = 0)$ and is orientated towards the coordinate origin [6, 19]

(a) $20 \cdot \log_{10} |D_{\mathrm{WFS}}(\alpha, \omega)|$

(b) $20 \cdot \log_{10} |D_{\mathrm{exact}}(\alpha, \omega)|$
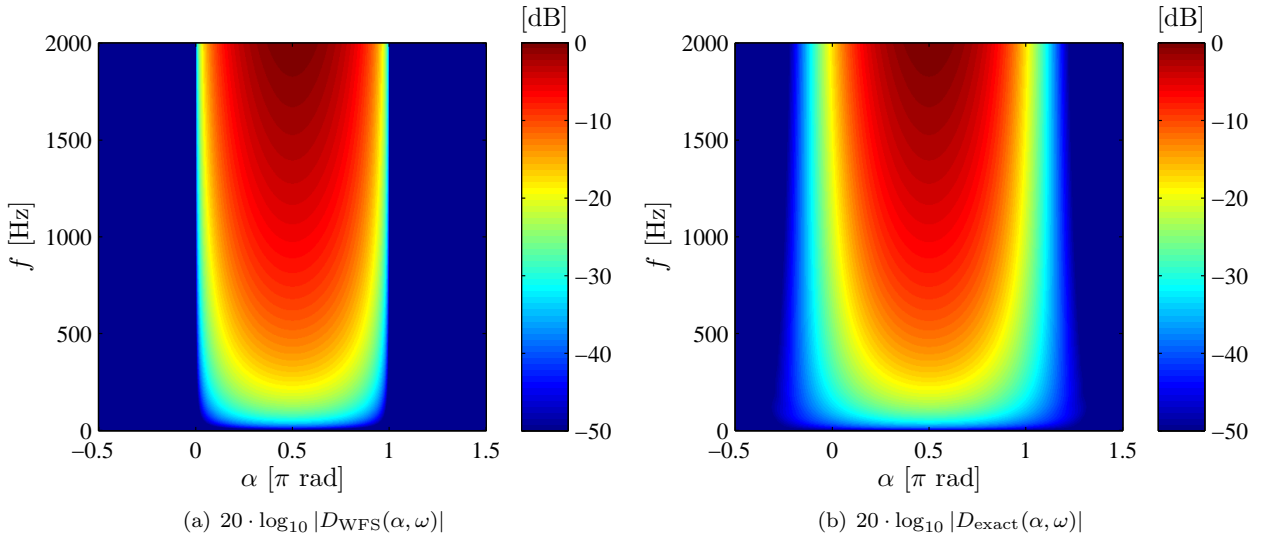
Fig. 3: $r_0 = 1.5$ m. The values are clipped as indicated by the colorbars.

From (12) and (1) we can deduce that

$$\mathring{D}_\nu(\omega) = \frac{1}{2\pi r_0} \frac{\mathring{P}_\nu(r, \omega)}{\mathring{G}_\nu(r, \omega)} = \qquad (13)$$

$$= \frac{1}{2\pi r_0} \frac{\breve{P}_\nu(\omega) \cdot J_\nu \left(\frac{\omega}{c} r \right)}{\breve{G}_\nu(\omega) \cdot J_\nu \left(\frac{\omega}{c} r \right)} \quad . \qquad (14)$$

For $J_\nu \left(\frac{\omega}{c} r \right) \neq 0$ the Bessel functions in (14) cancel out directly. Wherever $J_\nu \left(\frac{\omega}{c} r \right) = 0$ de l'Hôpital's rule [20] can be applied to proof that the Bessel functions also cancel out in these cases, thus making $\mathring{D}_\nu(\omega)$ and therefore also $D(\alpha_0, \omega)$ independent from the receiver position.
Introducing the result into (1) finally yields the secondary source driving function $D(\alpha_0, \omega)$ for a secondary source situated at position $\mathbf{x}_0$ reproducing a desired sound field with expansion coefficients $\breve{P}_\nu(\omega)$ reading

$$D(\alpha, \omega) = \frac{1}{2\pi r_0} \sum_{\nu=-\infty}^{\infty} \frac{\breve{P}_\nu(\omega)}{\breve{G}_\nu(\omega)} e^{j\nu\alpha} \, , \qquad (15)$$
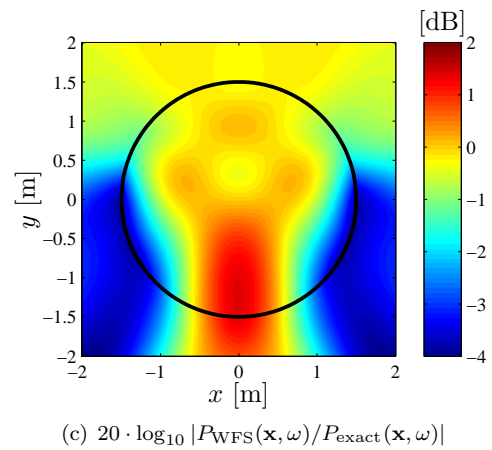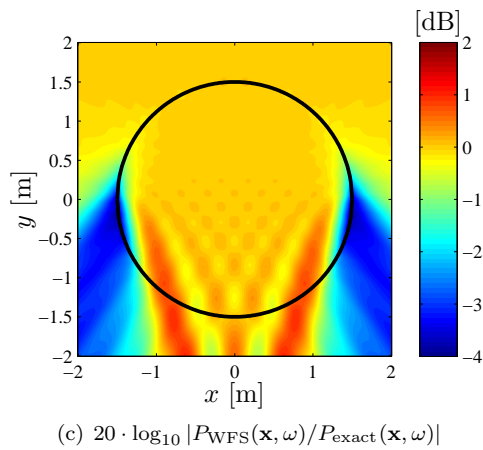
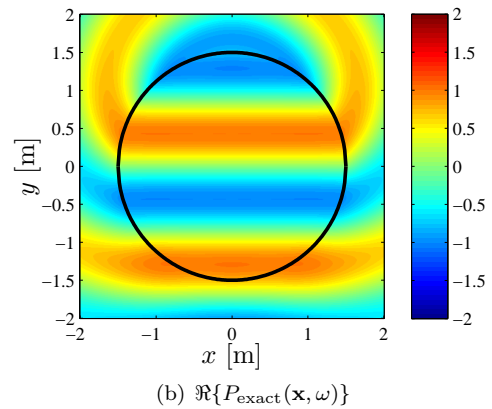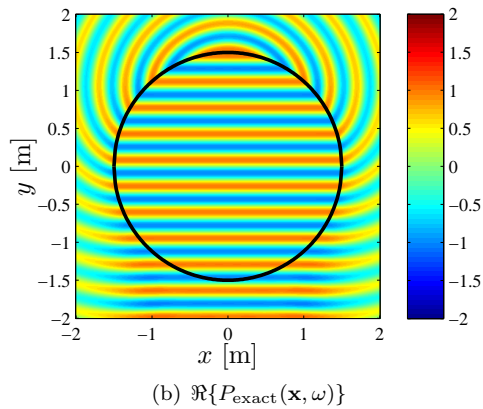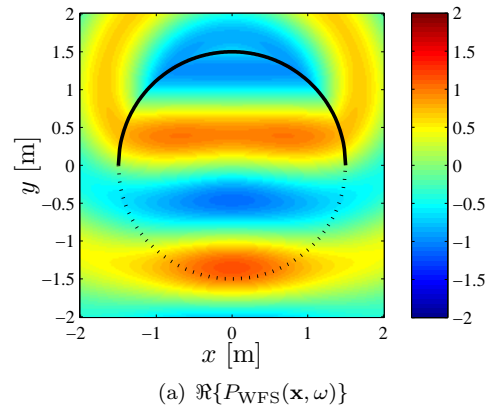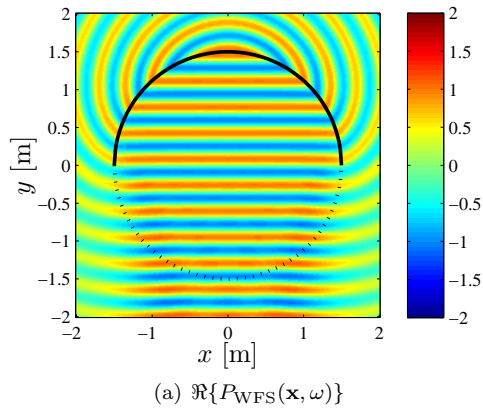whereby we omitted the index 0 in α_0.
Equation (15) can be verified by inserting it into (11). After introducing the Fourier series expansion of the secondary source sound fields according to (1), exchanging the order of integration and summation,

and exploitation of the orthogonality of the circular harmonics $e^{j\nu\alpha}$ [8] one arrives at the Fourier series expansion of the desired sound field, thus proving perfect reproduction. Note however that the coefficients $\breve{P}_\nu(\omega)$ respectively $\breve{G}_\nu(\omega)$ are typically derived from interior expansions. This implies that the desired sound field is only correctly reproduced inside the secondary source distribution.
We assume monopole line sources in the remainder of this paper in order to stay compatible with wave field synthesis. The secondary sources' spatio-temporal transfer function $G(\mathbf{x} - \mathbf{x}_0, \omega)$ of the source at position $\mathbf{x}_0$ is then given by the zero-th order Hankel function of second kind $\frac{j}{4} H_0^{(2)} \left(\frac{\omega}{c} |\mathbf{x} - \mathbf{x}_0| \right)$ [8].
The explicit driving function $D_{\mathrm{exact}}(\alpha, \omega)$ in order to reproduce a virtual plane wave with propagation direction θ_{pw} is given by [9]

$$D_{\mathrm{exact}}(\alpha, \omega) = -\frac{2j}{\pi r_0} \sum_{\nu=-\infty}^{\infty} \frac{j^{-\nu}}{H_\nu^{(2)} \left(\frac{\omega}{c} r_0 \right)} e^{j\nu(\alpha_0 - \theta_{\mathrm{pw}})} \, . \tag{16}$$

The infinite summation in (16) can of course not be performed in practical implementations. Therefore, in such practical implementations a truncation of the order is performed. However, we are primarily interested in theoretic fundamentals and therefore assume that enough addends are used so that no

(a) $\Re\{P_{\text{WFS}}(\mathbf{x},\omega)\}$

(a) $\Re\{P_{\text{WFS}}(\mathbf{x},\omega)\}$

(b) $\Re\{P_{\text{exact}}(\mathbf{x},\omega)\}$

(b) $\Re\{P_{\text{exact}}(\mathbf{x},\omega)\}$

(c) $20 \cdot \log_{10} |P_{\text{WFS}}(\mathbf{x},\omega)/P_{\text{exact}}(\mathbf{x},\omega)|$

(c) $20 \cdot \log_{10} |P_{\text{WFS}}(\mathbf{x},\omega)/P_{\text{exact}}(\mathbf{x},\omega)|$

Fig. 5: $f = 1000$ Hz, $r_0 = 1.5$ m. Solid lines in (a) and (b) indicate active secondary sources, dotted lines in (a) indicate inactive secondary sources.

Fig. 6: $f = 200$ Hz, $r_0 = 1.5$ m. Solid lines in (a) and (b) indicate active secondary sources, dotted lines in (a) indicate inactive secondary sources.

considerable error arises.

4. RESULTS

In the following subsection, we compare WFS and the exact solution in the scenario of a virtual plane wave with propagation direction $\theta_{\mathrm{pw}} = -\frac{\pi}{2}$ and given temporal frequency when it is reproduced by a continuous circular distribution of secondary monopole line sources.

4.1. Temporal frequency domain

Fig. 3 shows the absolute value of the WFS driving function $D_{\mathrm{WFS}}(\alpha, \omega)$ and of the exact driving function $D_{\mathrm{exact}}(\alpha, \omega)$ on a logarithmic scale. Both driving functions look very similar whereby the energy of the WFS driving function is confined to the interval $0 < \alpha < \pi$. The energy of the exact solution is not zero outside the above given angles. In other words, the exact solution requires all loudspeakers to be active whereby the "rear" secondary sources radiate substantially less energy than the "frontal" secondary sources. Note that the frontal loudspeakers represent the illuminated region in the equivalent scattering problem, the rear loudspeakers represent the shadowed area (Sec. 3.4).

4.2. Angular frequency domain

In order to get more insight into the properties of WFS we present an analysis of the reproduced sound fields of WFS and the exact solution in the angular frequency domain. The angular frequency domain is a suitable tool for this purpose because it allows to investigate signals with a broad temporal bandwidth and to deduce findings related to the spatial distribution of the artifacts in the reproduced sound field at the same time.
Recall (12) which holds for both WFS and the exact solution. It shows that the angular spectrum reproduced sound field $\mathring{P}_\nu(\omega)$ can be determined by a product of the angular spectrum of the driving function $\mathring{D}_\nu(\omega)$ and the angular spectrum of the secondary source at $\alpha = 0$, $\mathring{G}_\nu(\omega)$.
The exact solution is directly available in the angular frequency domain in (16). The WFS driving function $D_{\mathrm{WFS}}(\alpha, \omega)$ can be transformed into the

angular frequency domain via the relation

$$\mathring{D}_{\nu,\mathrm{WFS}}(\omega) = \frac{1}{2\pi} \int\limits_0^{2\pi} D_{\mathrm{WFS}}(\alpha, \omega) \, e^{-j\nu\alpha} \qquad (17)$$

For convenience, we perform the integration in (17) numerically. Such is numerical integration constitutes a discretization of the integral contour and can therefore cause aliasing. It was shown in [21] that it is impossible to perform the discretization of a circular contour without creating aliasing. However, when the number of sampling points is larger than a certain threshold, the energy of the aliasing contributions is very low and the operation is said to be aliasing-free. The required minimum number of sampling (i.e. integration) points is determined as follows.
From the well-known relation $\nu_{\max} = \lceil \frac{\omega}{c} r_0 \rceil$, e.g. [22], we can determine the highest required order $\nu_{\max}$ in order accurately reproduce a sound field with wavenumber k over the entire receiver area. In order that the repetitions in angular frequency domain which occur due to the discretization do not overlap and corrupt the region of interest we need at least $N_{\min} = 2\nu_{\max} + 1$ sampling points [21].
Fig. 4 depicts the ratio of the angular spectrum WFS and the the angular spectrum of the exact solution. It can be seen than for a given temporal frequency f and above a certain angular frequency, the energy of the WFS driving function is lower than the energy of the exact driving function. The ratio then rises quickly for even higher angular frequencies. The locations where the ratio is very high are not of primarily interest since the absolute energy of the driving function is very low and furthermore, these locations (high orders) primarily describe receiver locations which are outside the secondary source distribution. The maximum angular frequency $\nu_{\max}$ which needs to be considered can again be determined via $\nu_{\max} = \lceil \frac{\omega}{c} r_0 \rceil$. $\nu_{\max}$ is indicated in Fig. 4 by the black lines.
We conclude that the WFS driving function coincides with the exact solution apart from high angular frequencies where the WFS driving function exhibits slightly less energy than required. This implies that the sound field reproduced due to the WFS driving function exhibits a slightly too low amplitude at locations close to the secondary source distribution.

4.3. Reproduced sound field

Equation (12) holds both for WFS and the exact solution. We therefore derive the actually reproduced sound field for both methods from (12) and (1). We only have to pay attention that we include enough summations in the sum in (1) that no considerable error arises for the temporal frequency under consideration due to truncation of the sum.

As outlined in Sec. 4.2, we expect too low energy in the sound field reproduced by WFS for locations close to the secondary source distribution, since it is the highest orders which are relevant which are corrupted. This is indeed evident in Fig. 5. A frequency of 1000 Hz is reproduced there. Some minor amplitude deviations of around 1 dB are apparent which are likely to be inaudible since it is expected that the influence of the reproduction room and alike cause more significant impairment. Note that a frequency of 1000 Hz constitutes a situation where the requirements for the application of the physical optics approximation are roughly fulfilled (Sec. 3.4).

For relatively low frequencies, we expect the impairment to be distributed over the entire listener area. This is due to the circumstance that at low frequencies, only a few low orders are relevant for the receiver area. If one or more of these few orders is corrupted, a great part of the receiver area is affected. This is indeed apparent in Fig. 6 where a frequency of 200 Hz is reproduced. Note that a frequency of 200 Hz constitutes a situation where the requirements for the application of the physical optics approximation are not fulfilled (Sec. 3.4).

It can be seen from Fig. 6(a) that the wave fronts reproduced by WFS are not perfectly plane and that there are amplitude deviations. From Fig. 6(c) it is evident that the amplitude deviations can be as high as several dB for the situation under consideration. It is worth noting that the deviations for a given temporal frequency f reduce with increasing size of the secondary source distribution under consideration. Refer to Fig. 7 which depicts are secondary source distribution of $r_0 = 3$ m reproducing a plane wave of 200 Hz. Note the different scaling compared to Fig. 5 and 6.

A small secondary source distribution like the one simulated in Fig. 5 and 6 can be considered as worst case.

5. CONCLUSIONS

We have presented an analysis of two-dimensional wave field synthesis (WFS) employing circular continuous distributions of omnidirectional secondary sources. The focus of the investigation was to the systematic error introduced by the fact that the WFS driving function assumes that the secondary sources to exhibit a spatio-temporal transfer function which is equal to the Neumann Green's function of the secondary source distribution under consideration. However, the employed secondary sources are typically modeled omnidirectional.

The major consequence of this mismatch in secondary source types are amplitude deviations in the reproduced sound field. For very small secondary source distributions these amplitude deviations are likely to be negligible for moderate and high frequencies. At low frequencies of around 100 Hz, a few dB of deviation arise.
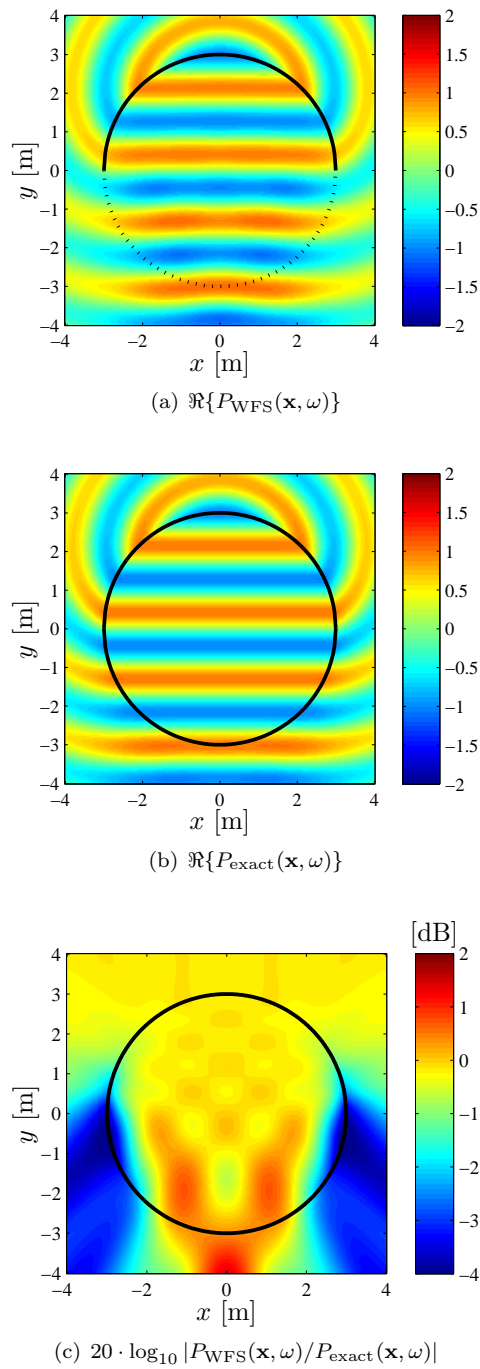
It was shown that the error decreases with increasing size of the secondary source distribution so that the investigated secondary source distribution with a radius of 1.5 m can be considered as a worst case. The above described findings are in accordance with the interpretation of WFS being a physical optics approximation of sound field reproduction.

It is likely that the properties of the reproduction room renders the amplitude deviations which occur at very low frequencies below a few hundred Hertz inaudible. If one nevertheless desires accurate reproduction, these problematic very low frequencies can be reproduced by means of Ambisonics techniques like e.g. [6] which provide a theoretically exact solution. Ambisonics techniques are computationally significantly more complex than WFS. However, at the targeted low frequencies, very accurate reproduction can be accomplished with a moderate number of modes keeping the processing cost low.

6. REFERENCES

[1] P. Vogel. Application of wave field synthesis in room acoustics. PhD thesis, Delft University of Technology, 1993.

[2] E. W. Start. Application of curved arrays in wave field synthesis. In *100th Convention of the AES*, Copenhagen, Denmark, May 11–14 1996.

[3] S. Spors, R. Rabenstein, and J. Ahrens. The theory of wave field synthesis revisited. In *124th Convention of the AES*, Amsterdam, The Netherlands, May 17–20 2008.

[4] M.A. Poletti. Three-dimensional surround sound systems based on spherical harmonics. *JAES*, 53(11):1004–1025, Nov. 2005.

[5] F.M. Fazi, P.A. Nelson, J.E.N. Christensen, and J. Seo. Surround system based on three dimensional sound field reconstruction. In *125th Conv. of the AES*, San Francisco, CA, Oct. 2–5 2008.

[6] J. Ahrens and S. Spors. An analytical approach to sound field reproduction using circular and spherical loudspeaker distributions. *Acta Acustica utd. with Acustica*, 94(6):988–999, Nov./Dec. 2008.

[7] Y. J. Wu and T. D. Abhayapala. Theory and design of soundfield reproduction using continuous loudspeaker concept. *IEEE Trans. on Audio, Speech, and Language Proc.*, 17(1):107–116, Jan. 2009.

[8] E. G. Williams. *Fourier Acoustics: Sound Radiation and Nearfield Acoustic Holography*. Academic Press, London, 1999.

[9] S. Spors and J. Ahrens. A comparison of wave field synthesis and higher-order Ambisonics with respect to physical properties and spatial sampling. In *125th Conv. of the AES*, San Francisco, CA, Oct. 2–5 2008.

[10] P. M. Morse and H. Feshbach. *Methods of Theoretical Physics*. Feshbach Publishing, LLC, Minneapolis, 1953.

[11] A. J. Berkhout. A holographic approach to acoustic control. *JAES*, 36:977–995, Dec. 1988.

[12] D. Colton and R. Kress. *Inverse Acoustic and Electromagnetic Scattering Theory*. Springer, Berlin, 1998.

[13] S. Spors. An analytic secondary source selection criteria for wave field synthesis. In *33rd German Annual Conference on Acoustics (DAGA)*, March 2007.

[14] E.W. Weisstein. Heaviside Step Function. MathWorld – A Wolfram Web Resource. http://mathworld.wolfram.com/HeavisideStepFunction.html, Retrieved July 09.

[15] F. Fazi, P. Nelson, and R. Potthast. Analogies and differences between 3 methods for sound field reproduction. In *Ambisonics Symposium*, Graz, Austria, June 25–27 2009.

[16] J. Daniel. Représentation de champs acoustiques, application à la transmission et à la reproduction de scènes sonores complexes dans un contexte multimédia. PhD thesis Université Paris 6, 2001.

[17] L. G. Copley. Fundamental results concerning integral representations in acoustic radiation. *JASA*, 44:28–32, 1968.

[18] B. Girod, R. Rabenstein, and A. Stenger. *Signals and Systems*. J.Wiley & Sons, 2001.

[19] J. Ahrens and S. Spors. Sound field reproduction employing non-omnidirectional loudspeakers. In *126th Conv. of the AES*, Munich, Germany, May. 7–10 2009.

[20] E.W. Weisstein. L'Hospital's Rule. MathWorld – A Wolfram Web Resource. http://mathworld.wolfram.com/LHospitalsRule.html, Retrieved Jan. 08.

[21] S. Spors and R. Rabenstein. Spatial aliasing artifacts produced by linear and circular loudspeaker arrays used for wave field synthesis. In *120th Convention of the AES, Paris, France*, May 20–23 2006.

[22] I. Balmages and B. Rafaeli. Open-sphere designs for spherical microphone arrays. *IEEE Trans. on Audio, Speech, and Language Proc.*, 15(2):727–732, Feb. 2007.

(a) $\Re\{P_{\mathrm{WFS}}(\mathbf{x}, \omega)\}$

(b) $\Re\{P_{\mathrm{exact}}(\mathbf{x}, \omega)\}$

(c) $20 \cdot \log_{10} |P_{\mathrm{WFS}}(\mathbf{x}, \omega)/P_{\mathrm{exact}}(\mathbf{x}, \omega)|$

Fig. 7: $f = 200$ Hz, $r_0 = 3$ m. Solid lines in (a) and (b) indicate active secondary sources, dotted lines in (a) indicate inactive secondary sources.